Regulators of G protein signaling RGS7 and RGS11 determine the onset of the light response in ON bipolar neurons

Yan Cao[a,1], Johan Pahlberg[b,1], Ignacio Sarria[a], Naomi Kamasawa[c], Alapakkam P. Sampath[b,2], and Kirill A. Martemyanov[a,2]

[a]Department of Neuroscience, The Scripps Research Institute, Jupiter, FL 33458; [b]Zilkha Neurogenetic Institute and Department of Physiology and Biophysics, University of Southern California, Los Angeles, CA 90089; and [c]Electron Microscopy Core Facility, Max Planck Florida Institute, Jupiter, FL 33458

Edited by King-Wai Yau, Johns Hopkins School of Medicine, Baltimore, MD, and approved April 3, 2012 (received for review February 9, 2012)

The time course of signaling via heterotrimeric G proteins is controlled through their activation by G-protein coupled receptors and deactivation through the action of GTPase accelerating proteins (GAPs). Here we identify RGS7 and RGS11 as the key GAPs in the mGluR6 pathway of retinal rod ON bipolar cells that set the sensitivity and time course of light-evoked responses. We showed using electroretinography and single cell recordings that the elimination of RGS7 did not influence dark-adapted light-evoked responses, but the concurrent elimination of RGS11 severely reduced their magnitude and dramatically slowed the onset of the response. In RGS7/RGS11 double-knockout mice, light-evoked responses in rod ON bipolar cells were only observed during persistent activation of rod photoreceptors that saturate rods. These observations are consistent with persistently high G-protein activity in rod ON bipolar cell dendrites caused by the absence of the dominant GAP, biasing TRPM1 channels to the closed state.

vision | retina | RGS proteins | signal transduction | synaptic transmission

G-protein signaling pathways play central roles in vertebrate vision. Phototransduction in photoreceptor cells use a well-studied G-protein signaling cascade to convert the absorption of light by visual pigments to an alteration in membrane potential (1). Across the synapse, ON bipolar cells (ON-BCs) also rely on G proteins to sense glutamate released from rod and cone photoreceptors. These cells use a metabotropic glutamate receptor, mGluR6 (2, 3), coupled through the heterotrimeric G protein $G\alpha_o$ (4, 5), to gate cationic TRPM1 channels (6–8). The hyperpolarizing light-evoked response of rod and cone photoreceptors reduces glutamate release, allowing TRPM1 channels to open and depolarize ON-BCs. Thus, $G\alpha_o$ deactivation appears to be the key molecular event in the mGluR6 cascade that leads to the generation of the ON-BC light-evoked response.

Although $G\alpha_o$ undergoes spontaneous deactivation, the rate of its intrinsic GTP hydrolysis that drives this process is too slow to account for the fast speed of the ON-BC light-evoked response, which occurs within hundreds of milliseconds. Members of the Regulator of G protein Signaling (RGS) protein family serve as GTPase accelerating proteins (GAPs) for the heterotrimeric G proteins. They stimulate the rate of the GTP hydrolysis on the Gα subunits thereby facilitating their deactivation (9). However, the identity of the dominant GAP in ON-BCs that shapes their light-evoked responses remains unknown.

Two members of the R7 subfamily of RGS proteins, RGS7 and RGS11, have been found to accumulate at the dendritic tips of ON-BCs, where they interact with mGluR6 (10–13). R7 RGS proteins form obligate trimers with their subunits Gβ5 and R7BP (or R9AP) (14). Knockout of Gβ5 eliminates the expression of all R7 RGS and completely abolishes the ON-BC responses to light concomitant with deficits in synapse formation (15). However, eliminating RGS11, R9AP, or R7BP, or partially disrupting RGS7 function, produces only minor deficits (10–13) that are inconsistent with their major role in $G\alpha_o$ inactivation.

In this study, we identify the key GAPs that ensure fast $G\alpha_o$ deactivation needed for the generation of rod ON-BC light-evoked responses. We generated RGS7 null mice completely devoid of RGS7 expression. Although the knockout of RGS7 produced no significant alteration in rod ON-BC light-evoked responses, concurrent elimination of RGS11 resulted in a severe reduction in light sensitivity without affecting the rod phototransduction cascade or synaptic connectivity between rods and rod ON-BCs. Furthermore, the time-to-peak of rod ON-BC responses to steps of bright light was ~40-fold longer than WT. These results indicate that the action of RGS7 and RGS11 is required for the generation of rod ON-BC light responses with high sensitivity and speed.

Results

To gain insight into the function of RGS7 in the mGluR6 cascade of ON-BCs, we generated a line of RGS7-knockout ($RGS7^{-/-}$) mice (Fig. 1). Our targeting strategy was based on elimination of the critical exon 4, which is expected to introduce a frameshift mutation, thereby truncating RGS7 in the middle of the N-terminal DEP domain and preventing the translation of critical functional elements of the protein (Fig. 1*A*). Indeed, retinas obtained from $RGS7^{-/-}$ mice contained no detectable RGS7 protein (Fig. 1*B*). This result is in contrast to previous attempts to eliminate RGS7 in mice, which used an RGS7 mutation with an internally truncated sequence that resulted only in partial reduction of its expression level (10–12). Notably, elimination of RGS7 reduced the level of short splice isoform of Gβ5 (Gβ5S) (Fig. 1*B*), suggesting the essential role of the association with RGS for the stability of this protein. Knockout of RGS7 also resulted in destabilization of R7BP, confirming the idea that both proteins exist in a complex in ON-BC dendrites (16). Importantly, knockout of RGS7 did not affect the expression of any other proteins essential for ON-BC light-evoked signaling (Fig. 1*B*). We further confirmed specific elimination of the RGS7 puncta in the outer plexiform layer of the retina using immunohistochemical staining (Fig. 1*C*).

Examination of the ON-BC function by single-flash electroretinography (ERG) revealed that the b-wave of the response that is thought to reflect the depolarizing activity of ON-BCs displayed similar sensitivity and time course in both wild-type (WT) and RGS7 knockouts (Fig. 1*D*). In addition, patch-clamp

Author contributions: A.P.S. and K.A.M. designed research; Y.C., J.P., I.S., and N.K. performed research; Y.C., J.P., I.S., N.K., A.P.S., and K.A.M. analyzed data; and A.P.S. and K.A.M. wrote the paper.

The authors declare no conflict of interest.

This article is a PNAS Direct Submission.

[1]Y.C. and J.P. contributed equally to this work.

[2]To whom correspondence may be addressed. E-mail: asampath@usc.edu or kirill@scripps.edu.

This article contains supporting information online at www.pnas.org/lookup/suppl/doi:10.1073/pnas.1202332109/-/DCSupplemental.

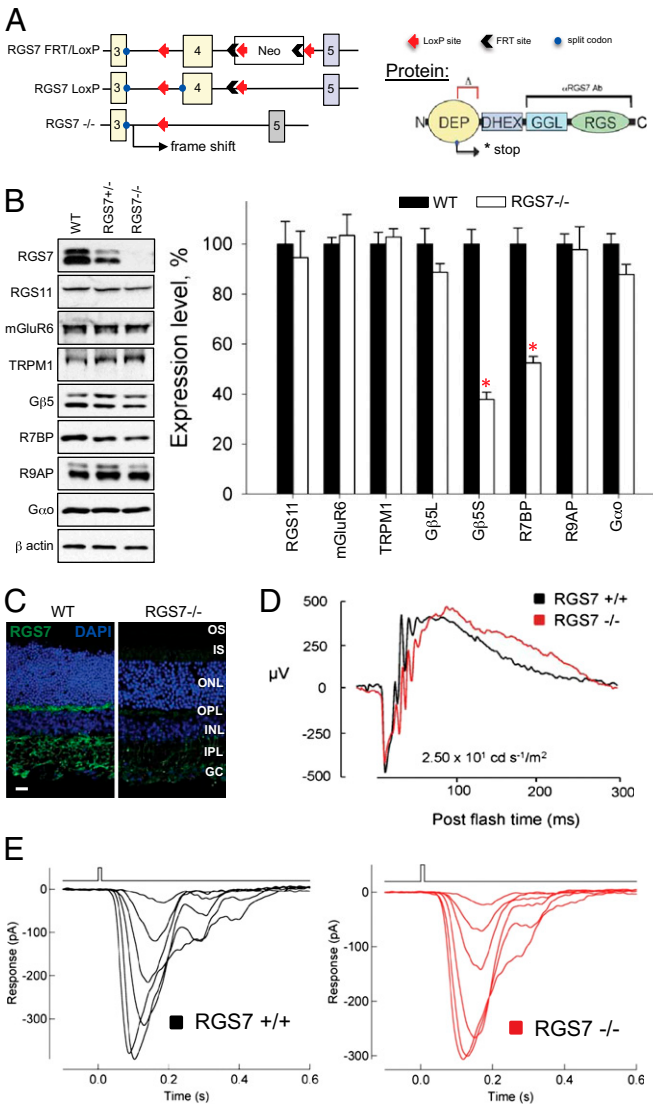

Fig. 1. Complete elimination of RGS7 preserves retina ON-BC responses to light. (*A*) Targeting exon 4 in the Rgs7 gene by homologous recombination is expected to truncate the protein in the middle of the DEP domain. (*B*) Western blot analysis of protein expression in mouse retinas. Knockout of RGS7 (RGS7$^{-/-}$) selectively reduces the levels of its interaction partners Gβ5 and R7BP ($P < 0.05$, *t* test; error bars are SEM values) without affecting the expression of proteins critical for the ON-BC function. Four retinas from separate mice in each case were used for the quantification. (*C*) RGS7 immunoreactivity is absent in the outer plexiform region of retina cross-sections. (Scale bar: 20 μm.) (*D*) RGS7-knockout mice display normal light responses as measured by ERG. A representative trace is shown out of four total experiments conducted with different mice, all yielding similar results. (*E*) Flash families of rod ON-BC responses in RGS7$^{-/-}$ mice display normal amplitude and response kinetics. Flash strengths were 0.4, 0.7, 1.4, 2.7, 5.5, and 11 activated rhodopsin (Rh*) per rod. Records are representative of data collected across four cells from one WT and nine cells from two RGS7$^{-/-}$ mice.

recordings from single-rod ON-BCs revealed no change in the magnitude or time course of the light-evoked response (Fig. 1*E*). Because the GTP hydrolysis on $G\alpha_o$ plays a profound role in the generation of the light response in the ON-BCs (17), elimination of the dominant GAP in these cells is expected to produce a strong phenotype, as demonstrated in similar studies on rod photoreceptors (18). We addressed the possibility of a functional compensation from other RGS proteins in ON-BCs, as suggested by earlier studies (10–12, 19). The dendritic tips of ON-BC are also known to contain RGS11, a protein that interacts with mGluR6 and shares similar structural organization with RGS7, including obligate association with Gβ5 (10–13). Consistent with the earlier observations (10–13), knockout of RGS11 in mice was not found to affect substantially ERG responses (Fig. S1), supporting our previous report that elimination of RGS11 alone does not affect light responses of rod ON-BCs (11).

To test the hypothesis that RGS11 masks the effects of RGS7 elimination, we generated double-knockout (DKO) mice lacking both RGS7 and RGS11 (RGS7$^{-/-}$RGS11$^{-/-}$; Fig. 2*A*). In these mice, all of the RGS7 and RGS11 immunoreactivity was eliminated from the dendritic tips of ON-BCs (Fig. 2*B*). Concurrent loss of RGS7 together with RGS11 further reduced the levels of Gβ5S, reinforcing the conclusion that these proteins form obligatory complexes (Fig. 2 *A* and *B*). Nevertheless, the expression of the main signal transducers, mGluR6, TRPM1, and $G\alpha_o$, remained unchanged. The cytoarchitecture of the DKO retinas was also normal (Fig. 2*C*). We found that rod ON-BCs from DKO retinas were no different from their WT littermates in overall morphology, dendritic branching, and the ability of the mGluR6 and TRPM1 to localize to the dendritic tips (Fig. 2*C*). Furthermore, dendritic tips of DKO ON-BCs were precisely aligned against the synaptic ribbon marker of the photoreceptors, CtBP2, in a manner indistinguishable from WT (Fig. 2*C*). Examination of the fine ultrastructure in DKO retinas by electron microscopy revealed the preservation of the intact synaptic triads containing bipolar cell dendrites reaching into the axonal arbor (spherule) of the rod photoreceptors (Fig. 2*D*). These data indicate that concurrent elimination of RGS7 and RGS11 did not affect the synaptic connectivity of the ON-BC.

Preservation of the synaptic connectivity allowed us to determine the functional consequences of simultaneous elimination of RGS7 and RGS11, as opposed to previous studies with Gβ5 knockouts, where synapses did not form during development (20). Light-evoked potentials (a-wave) measured by ERG (Fig. S2) and rod outer segment photocurrents measured with suction electrodes (Fig. S3) revealed rod responses that were indistinguishable from WT, suggesting that genetic manipulations did not affect the phototransduction cascade. However, the dark-adapted ERG b-wave was completely absent in DKO mice across a wide range of the light intensities (Fig. 3). Although the ERG may not allow the slow depolarizing activity of ON-BCs to be separated unambiguously from other ERG components, the no–b-wave phenotype suggests that a depolarizing response in DKO ON-BCs fails to develop on the fast timescale of WT ON-BC responses.

To characterize quantitatively alterations in ON-BC activity, single-cell recordings of light-evoked currents for scotopic stimuli (activating only rods) were made in rod ON-BCs (Fig. 4), a subclass of ON-BC in the mammalian retina that receives the predominant output of rod photoreceptors (21). Voltage-clamp recordings ($V_m = -60$ mV) revealed no detectable flash response in the rod ON-BCs from DKO retinas, consistent with ERG measurements, despite the preservation of normal responses in neighboring OFF bipolar cells that use other mechanisms for synaptic transmission (Fig. 4*B*). We hypothesized that a short reduction of synaptic glutamate concentration during a flash response might not reduce G-protein activity sufficiently to open TRPM1 channels. We therefore recorded the responses of the dark-adapted rod ON-BCs during a 20-s step of brighter light [~2,400 activated rhodopsin (Rh*) per rod per s] (Fig. 4 *C* and *D*) that prolongs the hyperpolarization of rods (22) and is thus expected to prolong the reduction in glutamate concentration. We found that these steps of brighter light produced responses in DKO rod ON-BCs that were much smaller in maximum amplitude (~10 pA) than the response of WT rod ON-BCs (which can exceed 500 pA) and displayed a time-to-peak of ~3 s (Fig. 4*E*).

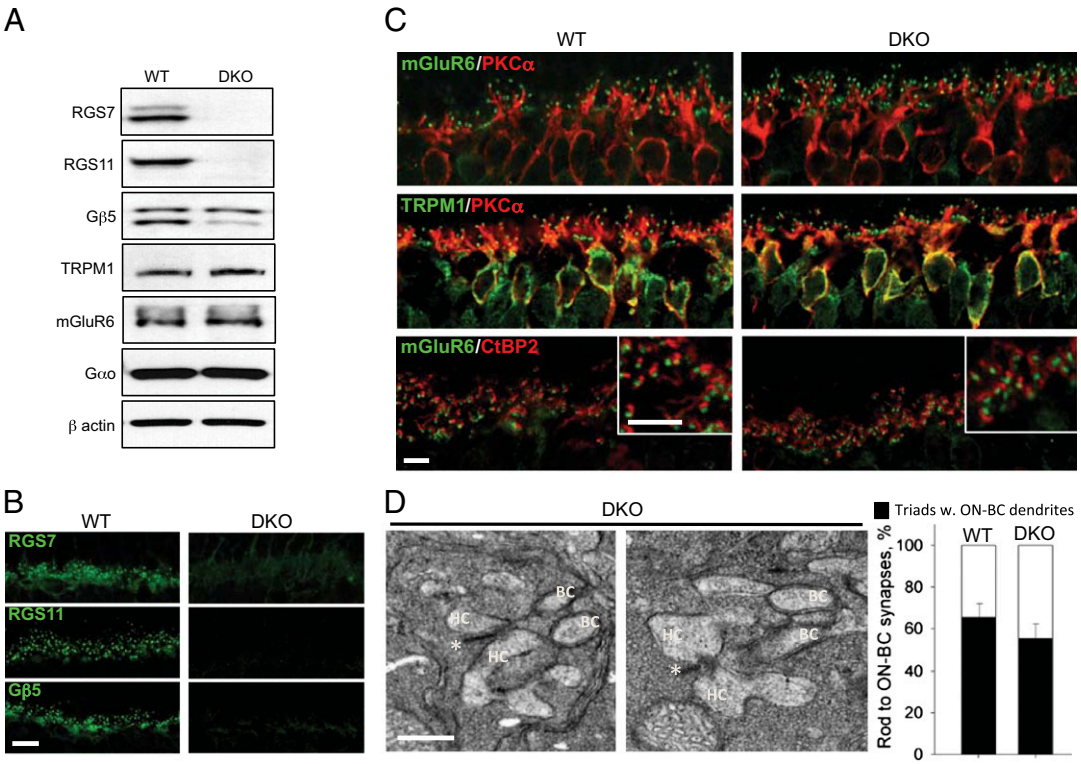

Fig. 2. Intact cytorachitecture and synaptic morphology in retinas of mice lacking both RGS7 and RGS11. (*A*) Western blot analysis of protein expression in mouse retinas. Concurrent knockout of both RGS7 and RGS11 does not affect the expression of the key ON-BC signaling proteins. Retinas from four mice were used for the quantification. (*B*) Retinas of RGS7,RGS11 DKOs completely lack RGS7-, RGS11-, and Gβ5-positive synaptic puncta in the outer plexiform layer. (Scale bar: 10 μm.) (*C*) Normal morphology, dendritic branching, and accumulation of mGluR6 and TRPM1 at the dendritic tips of the ON-BC in DKO retinas. Only bipolar cells and outer plexiform layer are shown. (Scale bar: 5 μm.) (*D Left*) Intact morphology of synapses between rods and horizontal/bipolar cells analyzed by electron microscopy. High magnification of the DKO synapses reveals the presence of the bipolar cell (BC) and horizontal cell (HC) dendrites within the rod spherules that contained intact ribbons (*). (Scale bar: 0.5 μm.) (*Right*) Quantification of synapses with all three identifiable features. Quantification results are based on preparations obtained from two separate mice for each genotype. For each genotype, 200–300 synaptic triads were scored by three independent investigators for the presence of ON-BC dendrites in the rod spherules. Error bars reflect deviation of the counts among the investigators.

The time-to-peak of WT rod ON-BCs was ~75 ms, 40-fold shorter than in the DKO rod ON-BCs. Such slowing of the rod ON-BC light-evoked response was not observed in RGS7$^{+/-}$ RGS11$^{+/-}$ mice (Fig. S4), despite reduced RGS protein concentration (Fig. 1*B*). Thus, elimination of both RGS7 and RGS11 relegated TRPM1 channels to a lower range of open probabilities and slowed opening to light stimuli. These results are consistent with high, persistent $G\alpha_o$ activity in rod ON-BC dendrites in darkness that increases saturation within the mGluR6 signaling cascade (17).

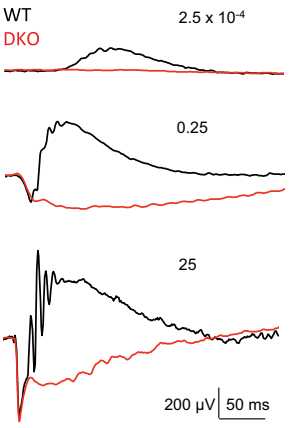

Fig. 3. Concurrent knockout of RGS7 and RGS11 causes no b-wave phenotype revealed by ERG. Mice lacking RGS7 and RGS11 (DKO) displayed normal a-waves but failed to generate b-waves on a fast timescale in response to flashes across broad range of light intensities. ERGs were recorded on dark-adapted mice. Each trace is a representative out of four recorded from separate WT and DKO mice. Numbers indicate light intensities of the flashes in cd·s/m^2.

Discussion

The time course of G-protein signaling is important for defining the functional properties of a signaling cascade. Here we have identified the key RGS proteins, RGS7 and RGS11, which serve as the dominant GAPs in rod ON-BCs. We show that their GAP activity endows these cells with the ability to mount a rapid response to the absorption of light in rod photoreceptors, a property that is key to the visual system's ability to detect fast changes in light intensity (23, 24). Accelerated light-evoked responses of ON-BCs with respect to rod photoresponses suggest that the speed of G-protein signaling, and the consequent turnover of second messengers, must be fast compared with phototransduction (17). What makes G-protein activity in ON-BCs different from other G-protein cascades, like phototransduction, is that the deactivation of $G\alpha_o$ produces the onset of the response rather than providing response termination. Thus, GAP proteins play a particularly important role in setting the speed of ON-BC responses.

Several previous studies have addressed the functional role of RGS proteins in the ON-BCs. The levels of both RGS7 and RGS11 are dramatically reduced in the retinas of Gβ5 knock-

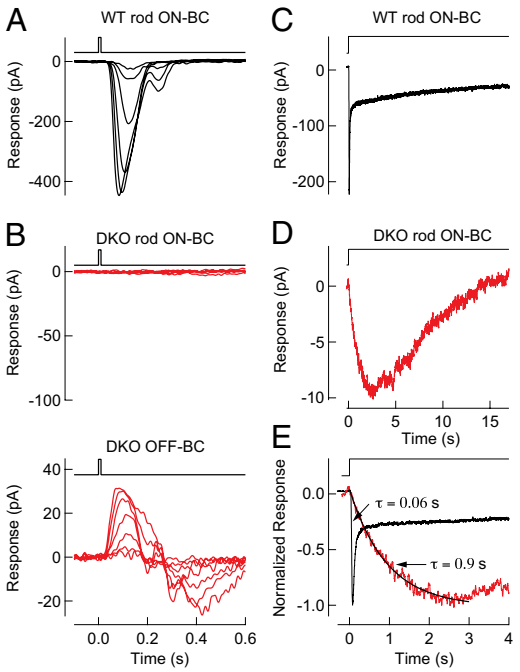

Fig. 4. Elimination of RGS7 and RGS11 slows the response of rod ON-BCs. (*A*) Light-evoked responses (black) to a 10-ms flash for a representative WT rod ON-BCs in voltage-clamp (V_m = −60 V). The flash monitor above the traces indicates the timing of the flash. Flash strengths were 0.4, 0.7, 1.5, 2.9, 5.9, and 11 Rh* per rod, with data collected across nine cells from two WT mice. (*B*, *Upper*) Absence of light-evoked responses (red) to 10-ms flashes for DKO rod ON-BC. (*Lower*) Viability of the retinal slice was confirmed by measuring light-evoked responses (red) in neighboring DKO OFF-BC. The flash monitor above the traces indicates the timing of the flash. Flash strengths were 0.4, 0.7, 1.5, 2.9, 5.9, 11, and 24 Rh* per rod. Records are representative of data collected across nine rod ON-BC and four OFF-BC cells from two DKO mice. (*C* and *D*) Light-evoked response (black) to a step of light producing 2,400 Rh* per rod per s averaged across seven voltage-clamped (V_m = −60 V) WT rod ON-BCs from one mouse (*C*) and averaged across seven voltage-clamped rod ON-BCs from two DKO mice (*D*; red). (*E*) Comparison of the time course of step responses in WT rod ON-BCs (black) and DKO rod ON-BCs (red). Exponential fits to rising phases revealed a time constant of ∼0.06 s in WT rod ON-BCs (not displayed) and ∼0.9 s in DKO rod ON-BCs. Membrane currents were low-pass filtered at 300 Hz and digitized at 1 kHz.

outs, for instance. However, gross neurological deficits observed in this model (25, 26) resulted in the malformation of the photoreceptor to ON-BC synapse and the predictable lack of the electroretinogram b-wave (20). Thus, the contribution of the RGS7 and RGS11 to the ON-BC light-evoked responses cannot be assessed in that model. Similarly, several groups used a strain of RGS7 mutant mice that was combined with the RGS11 null (10–12). These studies documented a 25-ms phase delay in the ERG b-wave with no change in the slope of the rising phase and no differences in light sensitivity. It should be noted that such observations are inconsistent with a dominant effect on $G\alpha_o$ activity, which would be expected to alter significantly the rising phase of light-evoked responses from ON-BCs. Indeed, biochemical characterization of this RGS7 mutant strain revealed the lack of RGS7 elimination and documented only partial disruption of the protein structure (10, 12). This finding suggests that the reduction in RGS7 function by the hypomorphic mutation was not sufficient to substantially alter the kinetics of the $G\alpha_o$ deactivation to the extent that it would limit the generation of the ON-BC responses. In contrast, the strain of RGS7-knockout mice used in this study is a complete null with a total elimination of RGS7 protein and hence with a complete abolishment of its GAP activity. In fact, our ERG recordings on RGS7-knockout mice document a similar small phase delay of the b-wave onset (Fig. 1*D*) that was seen in previous studies with RGS7 mutant strain only upon concurrent elimination of RGS11 (10–12). It should be noted that the minor phase delay observed in our ERG recordings does not reflect changes in rod ON-BC light-evoked responses (Fig. 1*E*). This finding further supports our conclusion that complete elimination of both RGS7 and RGS11 is required to reduce the level of GAP activity to the extent that it would rate-limit $G\alpha_o$ deactivation and hence affect both the sensitivity and the time course of the ON-BC responses. In parallel with this work, another study recently reported a lack of ON-BC signaling in a different mouse line lacking both RGS7 and RGS11 (27). In agreement with our findings, these mice also exhibited no detectable ERG b-wave at short times after the delivery of a bright flash. Although both of our studies observed a substantial number of normally formed synaptic triads, quantitative comparisons suggest that the other mouse model suffers from morphological deficits in the outer plexiform layer, a difference that might be explained by variations in the genetic manipulations and/or the strain background.

The increases in G-protein activity expected from the loss of the dominant GAP would be predicted to increase the extent of saturation within rod ON-BCs (17). This increase in saturation would further bias TRPM1 channels to their closed state, requiring larger and longer decrements in G-protein activity to open channels. We found that in darkness DKO rod ON-BCs exhibited this increase in saturation. Light-evoked responses of DKO rod ON-BCs were different from WT in two important ways. First, DKO rod ON-BCs lacked discernable responses to flashes of light that produced transient reductions in synaptic glutamate, indicating dramatically reduced light sensitivity. Second, the onset of the response was much slower in DKO than in WT rod ON-BCs, indicative of the slower deactivation of $G\alpha_o$ and consequently slow development of the depolarizing ON response. These features are consistent with the increased dark-adapted G-protein activity and match the predicted consequences expected upon the elimination of the dominant GAP in the rod ON-BC signaling cascade.

It should be noted that the ∼3-s time-to-peak of the step response of DKO rod ON-BCs is still much faster than would be expected if GAP activity were eliminated entirely, because $G\alpha_o$ inactivates in vitro with a time constant of ∼30 s (28). Given the promiscuous nature of RGS–G-protein interactions (9, 28), other proteins in rod ON-BCs may provide some residual GAP activity in the absence of RGS7 and RGS11. For instance, proteins like RetRGS1 (19) may still contribute to the fine regulation of the mGluR6 signaling in rod ON-BCs. The regulation of $G\alpha_o$ inactivation in other classes of cone ON-BCs may also differentially require the activity of RGS7, RGS11, or other RGS proteins. The mechanisms providing fine regulation of these mGluR6 signaling cascades remain to be determined.

Materials and Methods

Mouse Strains, DNA Constructs, and Antibodies. RGS7-knockout mice were generated by homologous recombination in hybrid 129/C57 ES cell lines following standard procedures. The targeting strategy included flanking exon 4 with LoxP sites and incorporating a neomycin resistance cassette, flanked by FLP recognition target (FRT) sites immediately downstream from exon 4 (Fig. 1). The targeting vector contained a long homology arm extending for ∼6 kbp upstream from exon 4 and a short homology arm with the ∼2-kbp sequence downstream from this exon. The recombination event was confirmed by Southern blotting with an internal probe, PCR, and by sequencing recombination and junction sites. To eliminate the FRT-flanked neomycin cassette in vivo, chimeric mice were bred with a germ-line FLP deleter strain B6.Cg-Tg(ACTFLPe)9205Dym/J (Jackson). Specificity of the cassette deletion was confirmed by PCR and sequencing. The resulting conditional RGS7 mice were crossed with a germ-line Cre-expressor strain B6.FVB-TgN(EIIa-Cre)C5379Lmgd (Jackson) to achieve elimination of exon 4 by LoxP recombination. Again, specificity of the deletion was confirmed by PCR

and sequencing. LoxP recombination eliminating exon 4 also resulted in the frameshift mutation as the amino acid is encoded across exon4/exon5 splice site. The resulting heterozygous mice were inbred to produce the homozygous constitutive RGS7 knockout.

The generation and characterization of RGS11-knockout mice was described (13). To generate RGS7/RGS11 DKOs, mice were crossed for two generations, and knockouts, as well as WT control littermates, were obtained from the double-heterozygote breeding pairs.

Electron Microscopy. Eyes were enucleated, cleaned of extraocular tissue, and prefixed for 15 min in cacodylate-buffered half-Karnovsky's fixative (11). The eyecups were hemisected along the vertical meridian and fixed overnight in the same fixative. The specimens were rinsed with cacodylate buffer (pH 7.4) and postfixed in 2% (vol/vol) osmium tetroxide (Electron Microscopy Sciences) in buffer for 45 min, gradually dehydrated in an increasing acetone series (25–100%), and embedded in Durcupan ACM resin (Electron Microscopy Sciences). Blocks were cut with 70-nm thickness and were stained with 6% aqueous uranyl acetate for 10 min and Sato's lead stain for 3 min. Sections were examined in a Tecnai G2 spirit BioTwin (FEI) transmission electron microscope at an 80-kV accelerating voltage. Images were captured with a Veleta CCD camera (Olympus) operated by TIA software (FEI). Quantification of the synaptic features was done by first identifying rod spherules with synaptic ribbons and adjacent processes of the horizontal cells. We then separately counted normal synaptic triads, which additionally contained rod bipolar dendrites juxtapositioned within the spherules, and abnormal triads, which did not appear to contain bipolar cell dendrites. Quantification was done by analysis of ~200–300 synapses for each genotype independently by three investigators.

Antibodies. The generation of rabbit anti-R9AP 144–223 (29), sheep anti-RGS9c (30), sheep anti-RGS6 (FL) (16), sheep anti RGS11 (CT) (16), rabbit anti-RGS11 (CT) (16), sheep anti-mGluR6 (31), and sheep anti-TRPM1 (31) were described. Rabbit anti-RGS7 (7RC1), anti-R7BP (TRS), and anti-Gβ5 (ATDG) were generous gifts from William Simonds (National Institute of Diabetes and Digestive and Kidney Diseases/National Institutes of Health, Bethesda). Rabbit anti-RGS7 (07-237; Upstate Biotechnology), mouse anti-β-actin (AC-15; Sigma), mouse anti-PKCα (ab11723; Abcam), mouse anti-CtBP2 (612044; BD Biosciences), and rabbit anti-Gαo (K-20; Santa Cruz Biotechnology) were purchased.

Preparation of Retina Lysates and Western Blotting. Whole retinas were removed from mice and lysed by sonication in ice-cold PBS supplemented with 150 mM NaCl, 1% Triton X-100, and Complete protease inhibitor tablets (Roche). Lysates were cleared by centrifugation at 20,800 × *g* for 15 min at 4 °C. Total protein concentration in the supernatant was measured by using a bicinchoninic acid protein assay kit (Pierce). Supernatants were added with SDS sample buffer (pH 6.8) containing 8 M urea and were subjected to 12.5% SDS/PAGE. Protein bands were transferred onto PVDF membranes, subjected to Western blot analysis by using HRP-conjugated secondary antibodies, and detected by using ECL West Pico system (Pierce). Signals were captured on film and scanned by densitometer, and band intensities were determined by using NIH ImageJ software.

Immunohistochemistry. Dissected eyecups were fixed for 15 min with 4% paraformaldehyde, cryoprotected with 30% sucrose in PBS for 2 h at room temperature, and embedded in optimal cutting temperature medium. Ten-micrometer frozen sections were obtained and blocked in PT1 (PBS with 0.1% Triton X-100 and 10% donkey serum) for 1 h, then incubated with primary antibody in PT2 (PBS with 0.1% Triton X-100 and 2% donkey serum) for 1 h. After four washes with PBS with 0.1% Triton, sections were incubated with fluorophore-conjugated secondary antibodies in PT2 for 1 h. After four washes, sections were mounted in Fluromount (Sigma). Images were taken with a Zeiss LSM 780 confocal microscope.

Single-Cell Electrophysiological Recordings from Rods and Rod ON-BCs. Mice were dark-adapted overnight and euthanized in accordance with protocols approved by the University of Southern California (Protocol 10890) and followed guidelines set by the National Institutes of Health on the care and use of animals. Rod photocurrents were measured with suction electrodes from outer segments protruding from clusters of dissociated tissue, and rod ON-BC (21) light-evoked currents were measured in whole-cell voltage-clamp recordings (V_m = −60 mV) from 200-μm-thick dark-adapted retinal slices as described (32–34). Retinal tissues were superfused with Ames' media equilibrated with 5% CO_2/95% O_2 and maintained at 35–37 °C. The internal solution for whole-cell recordings consisted of (in mM): 125 K-Aspartate, 10 KCl, 10 Hepes, 5 *N*-methyl-D-glucamine (NMG)–*N*-(2-hydroxyethyl)ethylenediamine-*N*,*N*,*N*-triacetic acid, 0.5 $CaCl_2$, 1 ATP·Mg, and 0.2 GTP·Mg; pH was adjusted to 7.2 with NMG·OH. Light responses were evoked with two types of stimuli: (*i*) 10- or 30-ms flashes from a blue LED (λ_{max} ~470 nm) or standard light bench (35), respectively, whose strength varied from producing a just-measurable response and increased by factors of two to three, were delivered to generate flash families; or (*ii*) longer steps of bright light were delivered to measure the response of rod ON-BCs when rod photoreceptors were persistently hyperpolarized (22). Membrane currents were filtered at 300 Hz by an 8-pole Bessel filter and digitized at 1 kHz.

ERG. Electroretinograms were recorded by using the UTA system and a Big-Shot Ganzfeld (LKC Technologies). Mice (4–8 wk old) were dark-adapted (≥6 h) and prepared for recordings by using dim red light. Mice were anesthetized with an i.p. injection of ketamine and xylazine mixture containing 100 and 10 mg/kg, respectively. All procedures were approved by the Institutional Animal Care and Use committee at the Scripps Florida Research Institute. Recordings were obtained from the right eye only, and the pupil was dilated with 2.5% phenylephrine hydrochloride (Bausch & Lomb), followed by the application of 0.5% methylcellulose. Recordings were performed with a gold loop electrode supplemented with contact lenses to keep the eyes immersed in solution. The reference electrode was a stainless steel needle electrode placed s.c. in the neck area. The mouse body temperature was maintained at 37 °C by using a heating pad controlled by ATC 1000 temperature controller (World Precision Instruments). ERG signals were sampled at 1 kHz and recorded with 0.3-Hz low-frequency and 300-Hz high-frequency cut-offs.

Full field white flashes were produced by a set of LEDs (duration < 5 ms) for flash strengths ≤2.5 cd·s/m^2 or by a Xenon light source for flashes > 2.5 cd·s/m^2 (flash duration < 5 ms). ERG responses were elicited by a series of flashes ranging from 2.5×10^{-4} to 2.5×10^{1} cd·s/m^2 in increments of 10-fold. Ten trials were averaged for responses evoked by flashes up to 2.5×10^{-1} cd·s/m^2, and three trials were averaged for responses evoked by 2.5×10^{0} cd·s/m^2 flashes. Single flash responses were recorded for brighter stimuli. To allow for recovery, interval times between single flashes were as follows: 5 s for 2.5×10^{-4} to 2.5×10^{-1} cd·s/m^2 flashes, 30 s for 2.5×10^{0} cd·s/m^2 flashes, and 180 s for 2.5×10^{1} cd·s/m^2 flashes.

ACKNOWLEDGMENTS. We thank Dr. William Simonds [National Institutes of Health (NIH)] for the generous gift of anti-Gβ5 antibodies and Ms. Natalia Martemyanova for performing genetic crosses needed to obtain mice used in these studies. This work was supported by NIH Grants EY018139 (to K.A.M.) and EY017606 (to A.P.S.) and by the McKnight Endowment Fund for Neurosciences (to A.P.S.).

1. Yau KW, Hardie RC (2009) Phototransduction motifs and variations. *Cell* 139:246–264.
2. Nakajima Y, et al. (1993) Molecular characterization of a novel retinal metabotropic glutamate receptor mGluR6 with a high agonist selectivity for L-2-amino-4-phosphonobutyrate. *J Biol Chem* 268:11868–11873.
3. Masu M, et al. (1995) Specific deficit of the ON response in visual transmission by targeted disruption of the mGluR6 gene. *Cell* 80:757–765.
4. Dhingra A, et al. (2000) The light response of ON bipolar neurons requires G[alpha]o. *J Neurosci* 20:9053–9058.
5. Nawy S (1999) The metabotropic receptor mGluR6 may signal through G(o), but not phosphodiesterase, in retinal bipolar cells. *J Neurosci* 19:2938–2944.
6. Koike C, et al. (2010) TRPM1 is a component of the retinal ON bipolar cell transduction channel in the mGluR6 cascade. *Proc Natl Acad Sci USA* 107:332–337.
7. Morgans CW, et al. (2009) TRPM1 is required for the depolarizing light response in retinal ON-bipolar cells. *Proc Natl Acad Sci USA* 106:19174–19178.
8. Shen Y, et al. (2009) A transient receptor potential-like channel mediates synaptic transmission in rod bipolar cells. *J Neurosci* 29:6088–6093.
9. Hollinger S, Hepler JR (2002) Cellular regulation of RGS proteins: modulators and integrators of G protein signaling. *Pharmacol Rev* 54:527–559.
10. Chen FS, et al. (2010) Functional redundancy of R7 RGS proteins in ON-bipolar cell dendrites. *Invest Ophthalmol Vis Sci* 51:686–693.
11. Zhang J, et al. (2010) RGS7 and -11 complexes accelerate the ON-bipolar cell light response. *Invest Ophthalmol Vis Sci* 51:1121–1129.
12. Mojumder DK, Qian Y, Wensel TG (2009) Two R7 regulator of G-protein signaling proteins shape retinal bipolar cell signaling. *J Neurosci* 29:7753–7765.
13. Cao Y, et al. (2009) Retina-specific GTPase accelerator RGS11/G beta 5S/R9AP is a constitutive heterotrimer selectively targeted to mGluR6 in ON-bipolar neurons. *J Neurosci* 29:9301–9313.
14. Anderson GR, Posokhova E, Martemyanov KA (2009) The R7 RGS protein family: multi-subunit regulators of neuronal G protein signaling. *Cell Biochem Biophys* 54: 33–46.
15. Chen CK, et al. (2003) Instability of GGL domain-containing RGS proteins in mice lacking the G protein beta-subunit Gbeta5. *Proc Natl Acad Sci USA* 100:6604–6609.

16. Cao Y, et al. (2008) Targeting of RGS7/Gbeta5 to the dendritic tips of ON-bipolar cells is independent of its association with membrane anchor R7BP. *J Neurosci* 28: 10443–10449.
17. Sampath AP, Rieke F (2004) Selective transmission of single photon responses by saturation at the rod-to-rod bipolar synapse. *Neuron* 41:431–443.
18. Chen CK, et al. (2000) Slowed recovery of rod photoresponse in mice lacking the GTPase accelerating protein RGS9-1. *Nature* 403:557–560.
19. Dhingra A, Faurobert E, Dascal N, Sterling P, Vardi N (2004) A retinal-specific regulator of G-protein signaling interacts with Galpha(o) and accelerates an expressed metabotropic glutamate receptor 6 cascade. *J Neurosci* 24:5684–5693.
20. Rao A, Dallman R, Henderson S, Chen CK (2007) Gbeta5 is required for normal light responses and morphology of retinal ON-bipolar cells. *J Neurosci* 27:14199–14204.
21. Dacheux RF, Raviola E (1986) The rod pathway in the rabbit retina: A depolarizing bipolar and amacrine cell. *J Neurosci* 6:331–345.
22. Okawa H, Sampath AP, Laughlin SB, Fain GL (2008) ATP consumption by mammalian rod photoreceptors in darkness and in light. *Curr Biol* 18:1917–1921.
23. Rieke F, Baylor DA (1998) Origin of reproducibility in the responses of retinal rods to single photons. *Biophys J* 75:1836–1857.
24. Bialek W, Owen WG (1990) Temporal filtering in retinal bipolar cells. Elements of an optimal computation? *Biophys J* 58:1227–1233.
25. Zhang JH, et al. (2011) Knockout of G protein β5 impairs brain development and causes multiple neurologic abnormalities in mice. *J Neurochem* 119:544–554.
26. Xie K, et al. (2012) Gβ5-RGS complexes are gatekeepers of hyperactivity involved in control of multiple neurotransmitter systems. *Psychopharmacology (Berl)* 219: 823–834.
27. Shim H, et al. (February 27, 2012) Defective retinal depolarizing bipolar cells (DBCs) in Regulators of G-protein Signaling (RGS) 7 and 11 double null mice. *J Biol Chem*, 10.1074/jbc.M112.345751.
28. Ross EM, Wilkie TM (2000) GTPase-activating proteins for heterotrimeric G proteins: Regulators of G protein signaling (RGS) and RGS-like proteins. *Annu Rev Biochem* 69: 795–827.
29. Keresztes G, Mutai H, Hibino H, Hudspeth AJ, Heller S (2003) Expression patterns of the RGS9-1 anchoring protein R9AP in the chicken and mouse suggest multiple roles in the nervous system. *Mol Cell Neurosci* 24:687–695.
30. Makino ER, Handy JW, Li TS, Arshavsky VY (1999) The GTPase activating factor for transducin in rod photoreceptors is the complex between RGS9 and type 5 G protein beta subunit. *Proc Natl Acad Sci USA* 96:1947–1952.
31. Cao Y, Posokhova E, Martemyanov KA (2011) TRPM1 forms complexes with nyctalopin in vivo and accumulates in postsynaptic compartment of ON-bipolar neurons in mGluR6-dependent manner. *J Neurosci* 31:11521–11526.
32. Armstrong-Gold CE, Rieke F (2003) Bandpass filtering at the rod to second-order cell synapse in salamander (Ambystoma tigrinum) retina. *J Neurosci* 23:3796–3806.
33. Sampath AP, et al. (2005) Recoverin improves rod-mediated vision by enhancing signal transmission in the mouse retina. *Neuron* 46:413–420.
34. Okawa H, et al. (2010) Optimal processing of photoreceptor signals is required to maximize behavioural sensitivity. *J Physiol* 588:1947–1960.
35. Miyagishima KJ, Cornwall MC, Sampath AP (2009) Metabolic constraints on the recovery of sensitivity after visual pigment bleaching in retinal rods. *J Gen Physiol* 134: 165–175.